J Polym Res (2016) 23: 124
DOI 10.1007/s10965-016-1014-5

ORIGINAL PAPER

Synthesis of polyaniline/mesoporous carbon nanocomposites and their application for CO_2 sorption

Mansoor Anbia[1] · **Samira Salehi**[1]

Received: 11 June 2015 / Accepted: 23 May 2016 / Published online: 1 June 2016

Abstract Ordered mesoporous carbons (OMC), were synthesized by nanocasting using ordered mesoporous silica as hard templates. Ordered mesoporous carbons CMK-1 and CMK-3 were prepared from MCM-48 and SBA-15 materials with pore diameters of 3.4 nm and 4.2 nm, respectively. Mesoporous carbons can be effectively modified for CO_2 adsorption with amine functional groups due to their high affinity for CO_2. Polyaniline (PANI)/mesoporous carbon nanocomposites were synthesized from in-situ polymerization by dissolving OMC in aniline monomer. The polymerization of aniline molecules inside the mesochannels of mesoporous carbons has been performed by ammonium persulfate. The nanocomposition, morphology, and structure of the nanocomposite were investigated by nitrogen adsorption-desorption isotherms, Fourier Transform Infrared (FT–IR), X-Ray Diffraction (XRD), Scanning Electron Microscopy (SEM) and thermo gravimetric analysis (TGA). CO_2 uptake capacity of the mesoporous carbon materials was obtained by a gravimetric adsorption apparatus for the pressure range from 1 to 5 bar and in the temperature range of 298 to 348 K. CMK-3/PANI exhibited higher CO_2 capture capacity than CMK-1/PANI owing to its larger pore size that accommodates more amine groups inside the pore structure, and the mesoporosity also can facilitate dispersion of PANI molecules inside the pore channels. Moreover, the mechanism of CO_2 adsorption involving amine groups is investigated. The results show that at elevated temperature, PANI/mesoporous carbon nanocomposites have a negligible CO_2 adsorption capacity due to weak chemical interactions with the carbon nanocomposite surface.

Keywords CO_2 adsorption · Polyaniline · Mesoporous carbon · CMK-3 · Nanocomposite

Introduction

Global warming caused by the emission of greenhouse gases has received worldwide concern since it probably brings severe environmental problems. Carbon dioxide (CO_2) is an important greenhouse gas, the concentration of which in atmosphere keeps growing and will continue to increase due to higher CO_2 emissions [1, 2]. It is produced from various industrial sources such as steel production, fossil fuel firing electric power generation, chemical and petrochemical plants [3]. Recently, CO_2 capture has attracted considerable attention as one of the options to reduce CO_2 emission.

Various efficient methods have been proposed for CO_2 capture for this purpose, including absorption, adsorption, cryogenic distillation and membrane [4, 5]. Traditionally, the large-scale capture of CO_2 produced from fossil-fuel combustion is based on the sorption by liquid amines such as monoethanolamine (MEA), diethanolamine (DEA), diglycol-amine (DGA), N-methyldiethanolamine (MDEA) and 2-amino-2-methyl-1-propanol (AMP) [6]. However, this technique has some disadvantages such as high energy consumption, solvent evaporation, limited cycling capacity, equipment corrosion, toxicity and flow problems caused by viscosity [7]. By contrast, adsorption process based on solid adsorbent can avoid those problems of traditional liquid absorption processes and presents lower energy requirement. The key point of this technology is to find the optimum, high

✉ Mansoor Anbia
anbia@iust.ac.ir

[1] Research Laboratory of Nanoporous Materials, Faculty of Chemistry, Iran University of Science and Technology, Narmak, Tehran 16846-13114, Iran

selectivity and high capacity solid sorbent. Different types of solid sorbents have been, or are currently being investigated as potential adsorbents for CO_2 capture, including metal oxides [8], zeolites [9], metal- organic frameworks (MOFs) [10], mesoporous silica [11] and carbon materials [12].

The adsorption capacity of zeolites largely declines in the presence of moisture in gas because of their highly hydrophilic character, thus necessitating very high regeneration temperatures (often above 300 °C). So that, they pose problems in practical field applications because of these additional recovery costs for their regeneration.

In contrast to zeolites, the structures of metal–organic frameworks (MOFs) can be controlled to a much higher degree through variations in the type and nature of the organic linkers and the metal centers. MOFs have good adsorption capacity for pure CO_2 at high pressure due to their high surface area. Their adsorption capacities are dramatically reduced when they are exposed to a gas mixture. Another concern which limits the widespread use of the MOFs in CO_2 capture is their low thermal and hydrothermal stabilities [13].

Mesoporous silica has a negative charge density due to the presence of Si-O and Si-OH groups, which makes it unsuitable for adsorption of CO_2 because of the fact that the residual hydroxyl groups on the pure silica surface are not able to induce sufficiently strong interactions and there are no specific adsorption sites.

Porous carbons are of particular interest in CO_2 adsorption due to their remarkable properties, such chemical inertness, excellent thermal/mechanical stability and hydrophobicity of their surface [14]. Most porous carbons are primarily microporous (According to the IUPAC classification, porous materials are divided into three classes: miroporous (<2 nm), mesoporous (2–50 nm) and macroporous (>50 nm)) [15–17]. In addition, conventional porous carbon has disadvantages, such as wide pore size distribution and an irregular pore structure. Therefore, there has been recently a considerable interest in the synthesis of ordered mesoporous carbons.

Mesoporous carbon with ordered pore structure, high specific surface area, large pore volume, tunable pore diameters and adjustable pore size disntribution can be prepared using the hard template method [18–20]. These ordered mesoporous carbons show great potential advantages over ordinary activated carbons and silica supports. Ryoo and co-workers synthesized mesoporous carbons CMK-1 and CMK-3 by carbonizing sucrose inside the pores of the cubic MCM-48 and hexagonal SBA-15 as hard templates [21]. Among the carbon sources, sucrose gives the easily reproducible results and gives the best structurally ordered framework. In the recent years, many efforts have been done to modify porous materials with various amine functional groups in order to obtain high CO_2 adsorption capacity and selectivity, in view of the high affinity and interaction between the amine groups and acidic gas.

The reaction of CO_2 with the amine occurs at room temperature to produce ammonium carbamates and can be released from the ammonium carbamates upon heating [22, 23].

Polyaniline (PANI) is one of the most important conducting polymers with high nitrogen content. This polymer has been intensively investigated in material science because of its ease of synthesis at low cost, good processability, high capacitive characteristics and environmental friendliness.

Ordered mesoporous carbon with regular and highly interconnected mesoporous channels can meet the demands of uniform dispersion of PANI molecules into the channels [24].

Nanocomposite of a conducting polymer with mesoporous carbon was mainly synthesized by in situ polymerization in solutions containing monomers of the conducting polymer and suspension of mesoporous carbon. Therefore, PANI/mesoporous carbon nanocomposite was prepared from a solution consisting of mesoporous carbon and aniline monomer. With addition of an oxidant solution containing $(NH_4)_2S_2O_8$, polymerization of aniline on the surface of mesoporous carbon occurs to form PANI/mesoporous carbon nanocomposite.

In the present work, mesoporous carbons CMK-1 and CMK-3 with different pore size distributions were prepared for the adsorption of CO_2 by MCM-48 and SBA-15. Then, polyaniline modified ordered mesoporous carbon, PANI/mesoporous carbon nanocomposite, was prepared through impregnation of OMC by aniline monomer. After amine modification, the amine groups become active chemisorption centers for higher amount of CO_2 adsorption. The structural order and textural properties of the adsorbents have been characterized by nitrogen adsorption-desorption isotherms, Fourier Transform Infrared (FT–IR), X-Ray Diffraction (XRD), Scanning Electron Microscopy (SEM) and thermo gravimetric analysis (TGA). CO_2 uptake capacity of the mesoporous carbon materials was obtained by a gravimetric adsorption apparatus for the pressure range from 1 to 5 bar and at the temperature ranging from 298 to 348 K. The CO_2 adsorption mechanism of the PANI/mesoporous carbon nanocomposite is proposed.

Experimental

Materials

All the chemicals used were of analytical grade from E. Merck (Germany), except nonionic triblock copolymer, $EO_{20}PO_{70}EO_{20}$ (Pluronic P123) that was from Aldrich (U.K.).

Synthesis of mesoporous silica (MCM-48)

Mesoporous silica (MCM-48) was synthesized, as reported by Shao et al. [25]. The MCM-48 samples were synthesized using tetraethyl orthosilicate (TEOS) as the silica source and

cetyltrimethylammonium bromide (CTAB) as template. In a typical synthesis, 10 mL of TEOS was mixed with 50 mL of deionized water, and the mixture was vigorously stirred for 40 min at 308 K, then 0.9 g of NaOH was added into mixture, and at the same time, 0.19 g of NaF was added into the mixture. After the NaF was added completely, the required amount of sources, respectively, were added. The solution was stirred for 60 min and 10.61 g of CTAB was added to the solution at one time, and stirring continued for 60 min. The resulting mixture was transferred into a stainless-steel autoclave maintained at 393 K under static conditions for 24 h for further condensation. A white precipitate was recovered by filtration and washed extensively with deionized water and dried in an oven at 373 K. The removal of the organic template was done by calcination in air at 823 K for 4 h (heating rate 1 °C/min) to obtain the MCM-48.

Synthesis of mesoporous silica (SBA-15)

SBA-15 was synthesized as described earlier [26]. The detailed procedure was as follows: first, 4 g P123 was dissolved in 150 mL H_3PO_4 solution at temperature 313 K. The resulting solution was transferred to a Teflon autoclave and then 9.6 mL of TEOS was added drop wise under stirring at 313 K and the mixture was stirred at 313 K for 24 h. The resulting mixture was aged at 373 K for 24 h without stirring. The produced solid product was obtained by filtration, then washed and dried at 373 K for 20 h. In order to remove the P123 template, the dried product was calcined under flow of air at 523 K for 3 h and at 823 K for 4 h.

Synthesis of mesoporous carbon (CMK-1)

CMK-1 was prepared using sucrose as a carbon source, MCM-48 material as template and sulfuric acid as carbonization catalyst. The preparation procedure of mesoporous carbon was as follows: 1 g of template (MCM-48) was impregnated with an aqueous solution obtained by dissolving 1.25 g of sucrose and 0.14 g of H_2SO_4 in 5 g of deionized water, keeping the mixture in an oven for 6 h at 373 K and subsequently at 433 K for another 6 h. In order to obtain fully polymerized and carbonized sucrose inside the pores of the silica template, 0.8 g of sucrose, 0.09 g of H_2SO_4 and 5 g of water were again added to the pretreated sample and the mixture was again subjected to the thermal treatment as described above. The color of the sample turned very dark-brown or nearly black. This powder sample was heated at 1173 K for 6 h under nitrogen to complete the carbonization. The silica template was then removed using 1 M NaOH solution of 50 % ethanol–50 % H_2O at 363 K. The template-free carbon product thus obtained was filtered, washed with ethanol and dried at 393 K.

Synthesis of mesoporous carbon (CMK-3)

For the preparation of CMK-3, a similar process to that of the CMK-1 was used and MCM-48 was replaced by SBA-15.

Synthesis of PANI/mesoporous carbon nanocomposites (CMK-1/PANI, CMK-3/ PANI)

Modification of the prepared mesoporous carbons was performed as follows: 2.55 g of mesoporous carbon was immersed in a solution containing 2.5 mL of aniline, 5 mL of 6 M hydrochloric acid and 50 mL of water. Following stirring for 30 min, an ammonium persulfate (APS) solution including 25 mL of water and 5.7 g of APS was added drop wise at 273 K and stirring continued for a further 3 h. The resulting precipitate was filtered and washed repeatedly with acetone, hydrochloric acid and deionized water, respectively. Finally the obtained sample was dried under vacuum at 373 K for 24 h.

Characterization

The porosity characteristics of the mesoporous carbon sorbents were determined by N_2 adsorption–desorption experiments performed at 77 K on micromeritics model ASAP 2010 sorptometer. The specific surface area (S_{BET}) was determined from the linear part of the Brunaure–Emmet–Teller (BET) equation. Pore size distribution was estimated from the adsorption branch of the isotherm by the Barrett–Joyner–Halenda (BJH) method.

The Fourier transform infrared spectra for the unmodified and modified samples were measured on a DIGILAB FTS 7000 instrument under attenuated total reflection (ATR) mode using a diamond module.

X-ray diffraction (XRD) was used to identify the crystal phases of the mesoporous carbon materials. These experiments were carried out on a Philips 1830 diffractometer equipped with Cu-Kα radiation. XRD patterns were obtained from 1° to 10° of 2θ, with a 2θ step size of 0.018° and a step time of 1 s.

The surface features and morphology of the materials were investigated by using scanning electron microscopy (SEM PHILIPS XL30). The samples were coated with gold in order to increase their conductivity before scanning.

Thermo gravimetric analysis was used to determine the thermal stability of the materials and was carried out from room temperature to 800 °C using a TGA/DTA (Mettler Toledo 851) analyzer at a heating rate of 10 °C/min under argon atmosphere.

CO_2 adsorption measurement

The carbon dioxide capacity of the synthesized materials was evaluated using volumetric method by setup shown in Fig. 1.

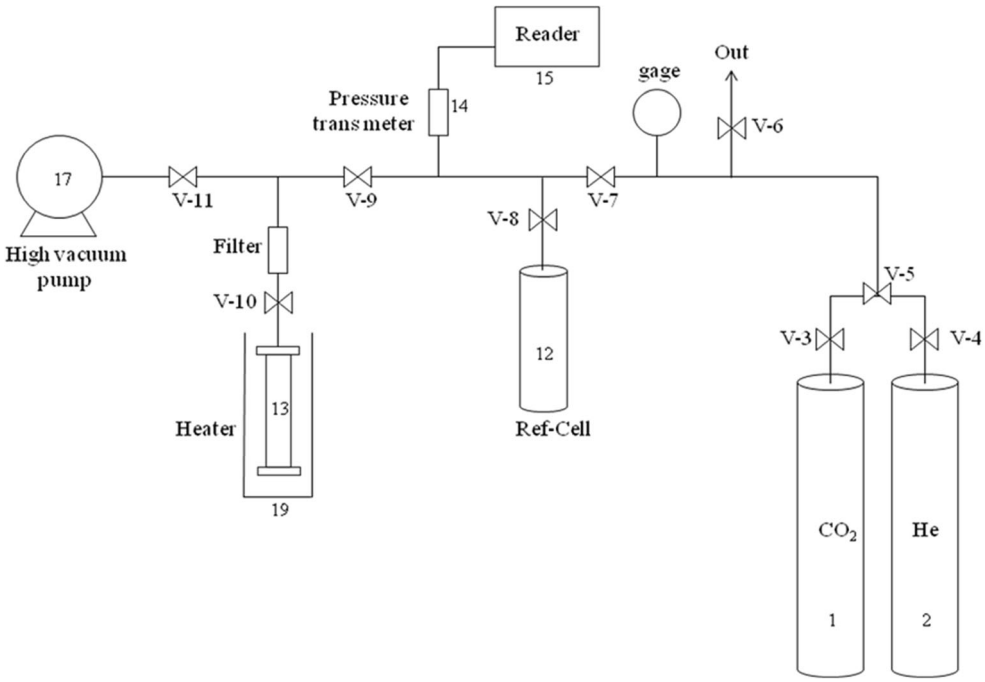

Fig. 1 Setup for adsorption capacity test

The volumetric method for carbon dioxide uptake measurements is extensively adopted because of its simplicity, low-cost, and easy assemblage. 1 g of sample was loaded inside the sample cell (13) and attached to the system. Then the system was carefully checked with the inert helium gas flow to ensure all connections have no leakage. The existing gas inside the system was swept out with helium. Afterwards, to remove residual solvents trapped in nanopores during synthesis, all the valves except 11, 10, 9 and 8 were closed and the system was vacuumed and heated at 473 K for 1.5 h. Ultra-high purity carbon dioxide (99.999 %) was introduced into adsorption unit for the CO_2 adsorption measurements. To perform an adsorption test, the valve of the CO_2 cylinder was opened and the CO_2 pressure was regulated at the desired value, then valves 7 and 8 were opened to reach a pressure balance in the reference cell (12). Afterwards, valve 10 was immediately opened and the pressure decrease was recorded. The pressure of adsorption cell decreased due to some dead volume and some CO_2 adsorption. The portion of dead volume was calculated via helium tests and subtracted from the total pressure change. Finally, the exact pressure decrease resulting from CO_2 adsorption could be calculated.

Results and discussion

Nitrogen adsorption-desorption isotherms analysis

The nitrogen adsorption-desorption isotherms of the mesoporous carbon samples are shown in Figs. 2 and 3. The obtained isotherms of the materials can be classified as type IV according to the IUPAC with capillary condensation indicating the existence of mesopores [27]. The specific surface area, the pore volume and average pore diameter of the unmodified and the modified mesoporous carbon materials were calculated from nitrogen isotherm data and are recorded in Table 1. The isotherm of CMK-1 shows an initial sharp uptake followed by a gradually increase up to about P/P_0 = 0.3–0.4.

Figure 3 illustrates the isotherms of CMK-3 and CMK-3/PANI. At low pressures, a steep increase is observed because of the formation of a monolayer on the pore walls, although at higher pressures an extended multilayer area and a sharp pore condensation step may be observed. The sharp inflection of the CMK-3 isotherm in P/P_0 range from 0.4 to 0.8 is

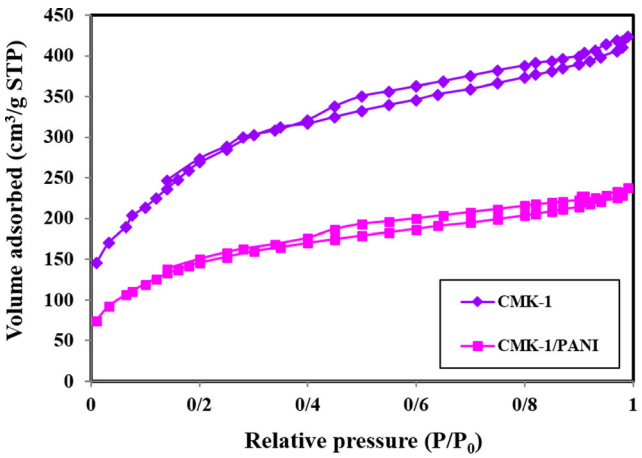

Fig. 2 Adsorption–desorption isotherms of nitrogen at 77 K on CMK-1 and CMK-1/PANI

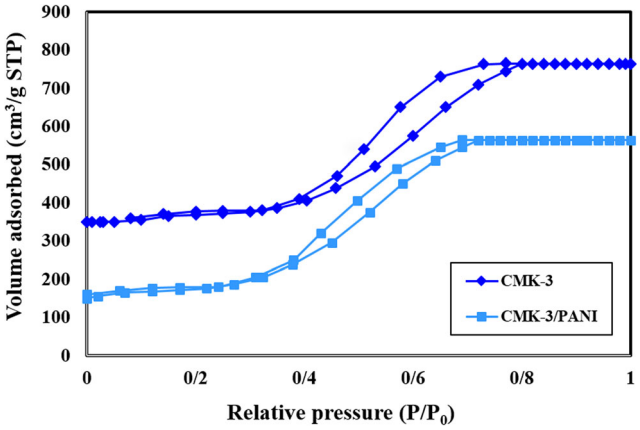

Fig. 3 Adsorption–desorption isotherms of nitrogen at 77 K on CMK-3 and CMK-3/PANI

characteristic of capillary condensation within uniform mesopores. The hysteresis loop of CMK-3/PANI shifts to lower pressure from CMK-3, indicating decrease of the pore diameter of this sample compared to the unmodified mesoporous carbon. The pore diameter of CMK-3 is 4.2 nm, which is larger than the pore diameter of CMK-1 (3.4 nm). This is to be expected, because the SBA-15 pore wall is thicker than that of MCM- 48, the CMK-3 pore size was larger than that of CMK-1. It is clear from Table 1 that the specific surface area, the pore volume and average pore diameter obviously decreased after modification due to surface coverage by PANI. As can be seen in Figs. 2 and 3, the nitrogen sorption isotherms of mesoporous carbon nanocomposites still featured pronounced type IV isotherms, indicating the preservation of the mesoporosity during the modification.

FT-IR analysis

The FT-IR technique was applied to monitor changes on the surface of the ordered mesoporous carbon and the content of the introduced PANI containing functional surface group. Figure 4 shows the FT-IR spectrum of mesoporous carbon materials over the range of 4000–400 cm^{-1}.

A broad band in the range of 3263–3542 cm^{-1} is seen which can be attributed to the O–H stretching bonds. A characteristic stretching vibration of C–O–C group at 1097 cm^{-1} appears in FT-IR spectrum of mesoporous carbon, which may be an important active site for interactions of polyaniline and mesoporous carbon in nanocomposite. In the spectra of CMK-1/PANI and CMK-3/PANI, the characteristic peaks at 1716 and 1616 cm^{-1} correspond to the quinoid ring and the benzene ring, respectively. Characteristics peaks at 1369, 1226 cm^{-1} and 815 cm^{-1} are observed in the IR spectrum of PANI/mesoporous carbon nanocomposites. These peaks can be attributed to the C–N stretching of the secondary aromatic amine, aromatic C–H in plane bending and out-of-plane C–H bending vibration, respectively. This result indicates that PANI was presented in the nanocomposites CMK-1/PANI and CMK-3/PANI.

Table 1 Textural properties determined from nitrogen adsorption-desorption experiments at 77 K

Adsorbent	S_{BET} (m^2 g^{-1})	Average pore size (nm)	V_p(cm^3 g^{-1})
CMK-1	1010	3.4	0.69
CMK-1/PANI	769	2.5	0.54
CMK-3	970	4.2	0.83
CMK-3/PANI	710	3.1	0.71

XRD analysis

The structure of the mesoporous carbon materials was studied using low angle XRD. Mesoporous carbon structures formed in the mesoporous silica template having two disconnected systems are also disconnected and are capable of changing their positions with respect to one another when the template is removed [28]. The XRD pattern for CMK-1 exhibits an intense diffraction peak and two weak peaks indexed as (1 1 0), (2 1 1), and (2 2 0) crystal facets, which belong to well-ordered cubic space group I4132 [29]. Higher order reflections are observed in the region 2 = 3.5–6.5°, which are a superposition of various reflections that are indexed according to the I4132 space group. The resulting XRD pattern for CMK-3 and CMK-3/PANI, obtained in the 2 range of 0.8–10° is presented in Fig. 5. These ordered mesoporous carbons are hexagonally mesostructures as evident from the presence of at least three peaks that can be indexed to the (100), (110) and (200) reflections of the two dimensional (2D) hexagonal space group p6mm. It should also be noted that the synthesized materials are a true replica of the parent mesoporous silica material SBA-15 [30]. The XRD patterns of both CMK-1 and CMK-3 indicate that two samples have highly ordered uniform mesopores. Weaker peaks of CMK-1/PANI and CMK-3/PANI compared to CMK-1 and CMK-3 can be due to the reduction of their crystallization. However, it should be emphasized that their primary structure of mesoporous carbon materials was retained (Fig 6).

SEM analysis

Scanning electron microscopy (SEM) images of mesoporous carbon samples, before and after modication, are shown in Fig. 7. SEM images of the mesoporous carbons both before and after modication show rod-like morphology. This

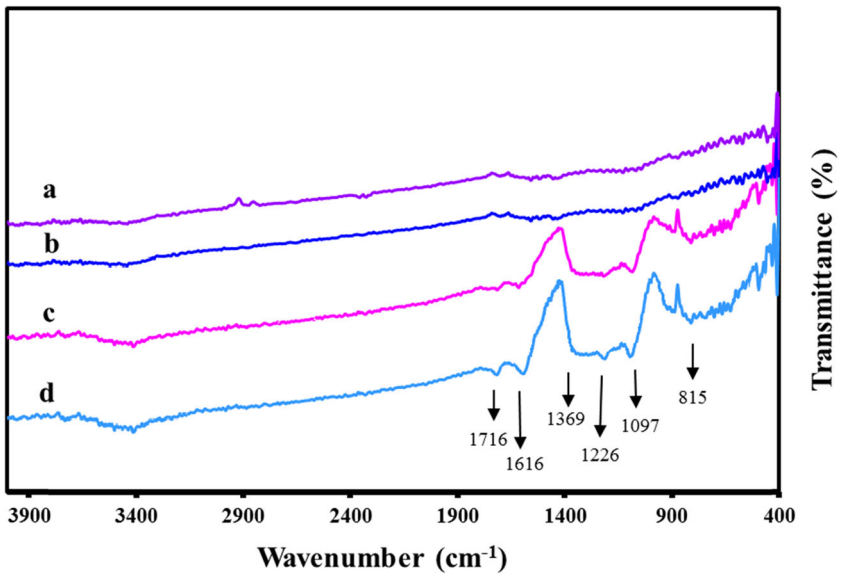

Fig. 4 FT-IR spectra of CMK-1 (**a**), CMK-3 (**b**) CMK-1/PANI (**c**) and CMK-3/PANI (**d**)

suggests that the shape of the structure is not changed after modification of the mesoporous carbons surface by PANI.

TGA analysis

In order to confirm the PANI content in the nanocomposite, the thermal analysis of the mesoporous carbon nanocomposite was investigated with TGA measurements. Thermogravimetric behaviors of mesoporous carbon materials recorded in thermal stability tests are shown in Fig. 8.

There are three major stages of weight loss for PANI as shown in Fig. 8 curve e. The first small fraction of weight loss from room temperature to about 120 °C arises mostly from the expulsion of absorbed water molecules. The second step for weight loss, from 180 °C to 300 °C, is due to the loss of acid dopant. Then a very significant weight loss occurs at about 400 °C due to thermal oxidative decomposition of polymer chain [31]. As shown in Fig. 8 curve a and b, ordered mesoporous carbons are very stable and no decomposition takes place until 800 °C. It is also important to note that the CMK-1/PANI nanocomposite does not have a distinct decomposition temperature and show a gradual weight loss with increasing temperature. The results imply good thermal stability of PANI in the nanocomposite because of diffusion constraints in the channel system [32]. The CMK-3/PANI exhibits similar weight change pattern, although at the same temperature shows higher weight loss. It can be concluded that the

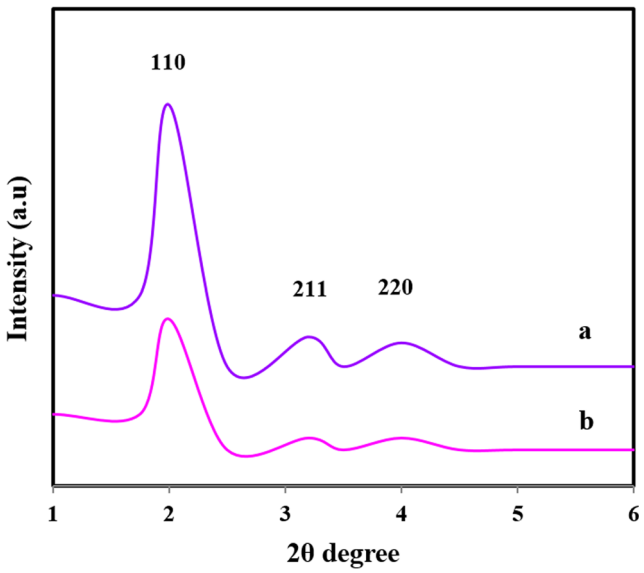

Fig. 5 XRD patterns of CMK-1 (**a**) and CMK-1/PANI (**b**)

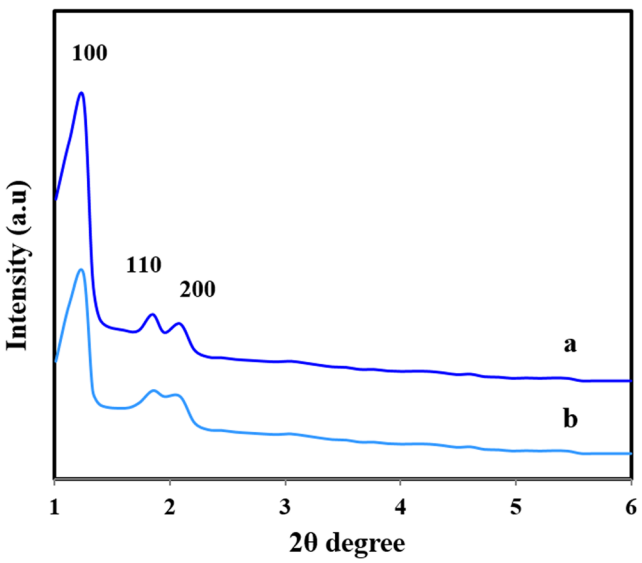

Fig. 6 XRD patterns of CMK-3 (**a**) and CMK-3/PANI (**b**)

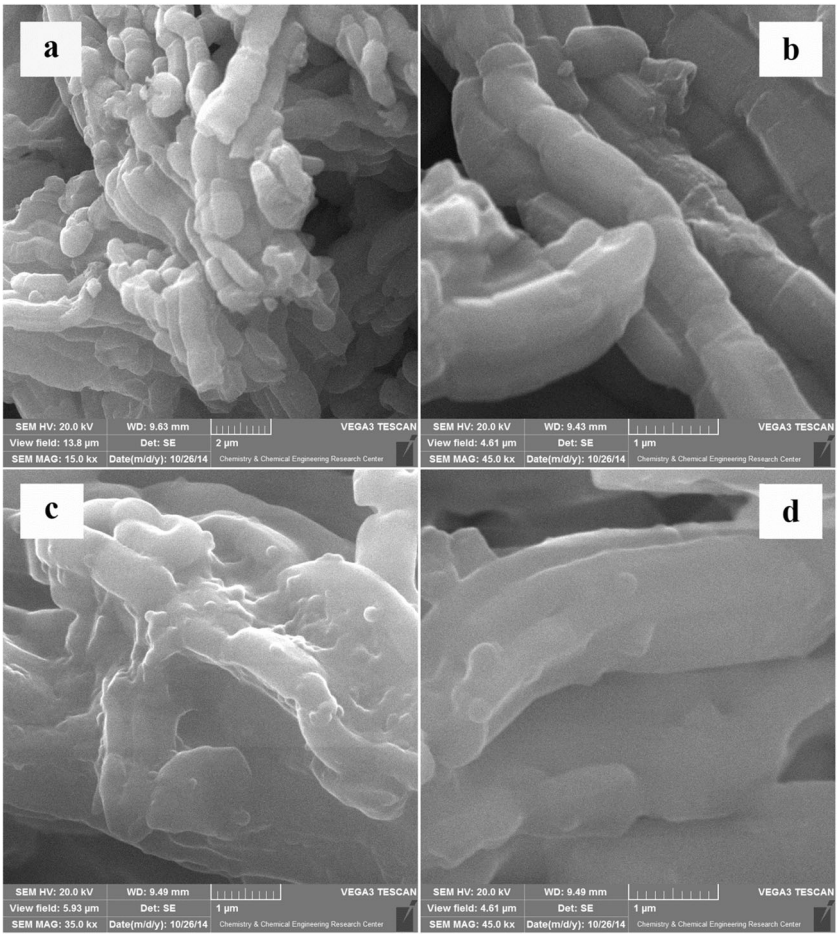

Fig. 7 SEM images of CMK-1 (**a**), CMK-3 (**b**), CMK-1/PANI (**c**) and CMK-3/PANI (**d**)

content of PANI in CMK-3/PANI is higher than CMK-1/PANI.

Isotherm of CO_2 adsorption

Figure 9 shows the CO_2 adsorption isotherms on mesoporous carbon materials at 298 K up to 5 bar. The adsorption capacity depends on the physical properties and surface chemical properties of the adsorbent. It can be seen from the Fig. 9 that, after coated with PANI, two mesoporous carbons show higher adsorption capacity than their initial materials. It should also be noted that the forces formed between PANI and CO_2 can be

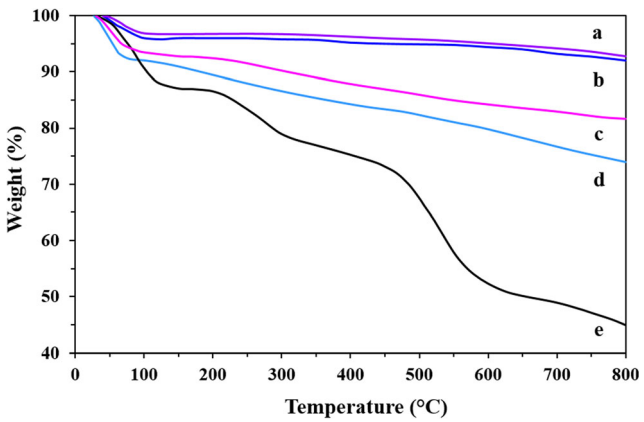

Fig. 8 TGA plots of CMK-1 (**a**), CMK-3 (**b**), CMK-1/PANI (**c**), CMK-3/PANI (**d**) and PANI (e)

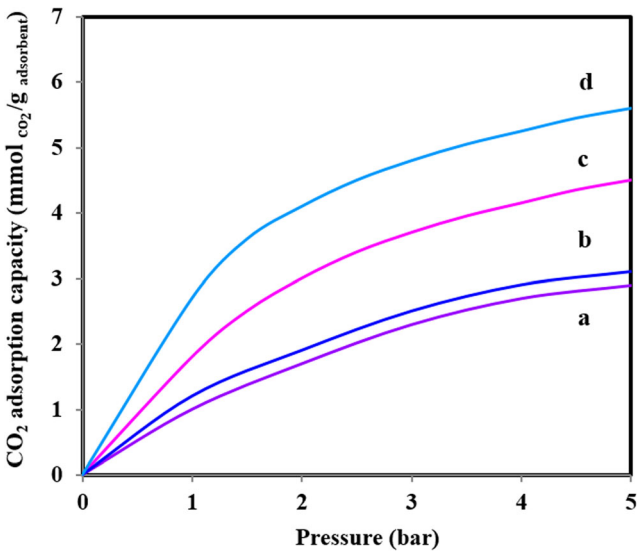

Fig. 9 CO_2 adsorption capacity of CMK-1 (**a**), CMK-3 (**b**), CMK-1/PANI (**c**) and CMK-3/PANI (**d**) at different pressures and 298 K

attributed to electrostatic interactions between the carbon of CO_2 and the nitrogen and the hydrogen bonding. The main factor comes from Lewis acid-Lewis base electrostatic interactions.

The CMK-1/PANI and CMK-3/PANI possess weak basic amine groups with lone pair of electrons on atom N. Thus, these electrons make nucleophilic attack on quadrupolar CO_2 molecule with more degree of positive charge on the C atom. The carbamate formed during CO_2 adsorption on amine group, constructs hydrogen bonds between nearby nitrogen atom of amine groups and active H atoms of chemisorbed CO_2 in order to stabilize the adsorbed CO_2. The results of Vogiatzis et al. seem to be in consistent with the results of this study [33].

It is important to note that CMK-3/PANI exhibits higher amount of CO_2 adsorption than that of CMK-1/PANI. It has become clear that the surface of the pores with smaller pore size cannot be utilized in modification and the fractional coverage of the small pore surface may depend on the length of the diffusion path [34]. In the adsorbent with smaller pores, CMK-1, pore blocking may occur due to aggregation of PANI molecules. Consequently, the long diffusion path in the small mesopores will lead to a greater possibility for pore blocking to occur, and therefore, a smaller loading is obtained in CMK-1. However, in the case of CMK-3, the large pore size facilitates the diffusion of the PANI molecules from the mesopore entrance to the inside part of the carbon, and pore blocking might not occur. Hence, it is assumed that the higher loading of PANI in CMK-3 carbon is due to the larger pore size CMK-3, which allows full access of the mesopores by the PANI molecules. Based on these results, it is suggested that amine and the pore size of mesoporous carbon play an important role in the CO_2 adsorption process. This obviously indicates that, the CMK-3/PANI has higher CO_2 capture capacities probably due to high amin groups (PANI), together with its large pore size.

In new kinds of adsorbents, determining the optimal adsorption temperature is important. The adsorption studies were carried out at 298, 323, and 348 K the results of these experiments are listed in Table 2. It can be seen that decrease in temperature generally increase the adsorption capacity and maximum adsorption capacity is noticed at 298 K which shows an exothermic adsorption. On increasing the temperature, adsorption capacity decreases, which could be because of the weak hydrogen bonding between CO_2 and amine hydrogen. These weak hydrogen bonds could restrain the freshly arriving CO_2, to interact with amine groups and therefore the chemisorption of CO_2. It is also important to note that, at high temperature, CO_2 molecules are activated with slightly higher kinetic energy in order that the appropriate molecular direction for nucleophilic attack might not be favorable, so adsorption capacity decreases.

Table 2 The effect of temperature on CO_2 adsorption in PANI/mesoporous carbon nanocomposites at 5 bar

Adsorbent	Temperature (K)	CO_2 adsorption capacity ($mmol_{co2}/g_{adsorbent}$)
CMK-1/PANI	298	4.5
	323	3.1
	348	2.4
CMK-3/PANI	298	5.6
	323	3.8
	348	2.9

Conclusions

Two types of mesoporous carbons have been synthesized from two types of mesoporous silica templates. MCM-48 and SBA-15 silica templates were synthesized to prepare mesoporous carbon supports CMK-1 and CMK-3, respectively. After coating with PANI, mesoporous carbon nanocomposites exhibited higher adsorption than their initial mesoporous carbons. That is due to the formation of electrostatic interaction between PANI on the mesoporous carbons surface and CO_2 molecules. The nanocomposition, morphology, and structure of the nanocomposite were investigated by nitrogen adsorption-desorption isotherms, Fourier Transform Infrared (FT–IR), X-Ray Diffraction (XRD), Scanning Electron Microscopy (SEM) and thermo gravimetric analysis (TGA). CO_2 uptake capacity of the mesoporous carbon materials were obtained by a gravimetric adsorption apparatus in the pressure range from 1 to 5 bar and at the temperature ranging from 298 to 348 K. The results of this study show that CMK-3/PANI nanocomposite, with a larger pore size and higher nitrogen content, has a higher CO_2 adsorption capacity than CMK-1/PANI. At room temperature, the high uptake is attributed to exothermic adsorption. When the temperature is increased to 348 K, some of physically captured CO_2 molecules escaped from the surface of the pore walls and thus the CO_2 adsorption capacity is decreased.

Acknowledgments The authors are thankful to Research Council of Iran University of Science and Technology (Tehran) and Iran National Science Foundation (INSF) for financial support to this study.

References

1. Li B, Duan Y, Luebke D, Morreale B (2013) Advances in CO_2 capture technology: a patent review. Appl Energy 102:1439–1447
2. Leung DY, Caramanna G, Maroto-Valer MM (2014) An overview of current status of carbon dioxide capture and storage technologies. Renew Sustain Energy Rev 39:426–443

3. Dantas TL, Luna FMT, Silva IJ, Torres AEB, de Azevedo DC, Rodrigues AE, Moreira RF (2011) Carbon dioxide–nitrogen separation through pressure swing adsorption. Chem Eng J 172:698–704
4. Lara-Medina J, Torres-Rodríguez M, Gutierrez-Arzaluz M, Mugica-Alvarez V (2012) Separation of CO_2 and N_2 with a lithium-modified silicalite-1 zeolite membrane. Int J Greenh Gas Control 10:494–500
5. Scholes CA, Ho MT, Wiley DE, Stevens GW, Kentish SE (2013) Cost competitive membrane—cryogenic post-combustion carbon capture. Int J Greenh Gas Control 17:341–348
6. Rochelle GT (2009) Amine scrubbing for CO_2 capture. Science: 1652–1654
7. Yeh JT, Resnik KP, Rygle K, Pennline HW (2005) Semi-batch absorption and regeneration studies for CO_2 capture by aqueous ammonia. Fuel Process Technol 86:1533–1546
8. Roesch A, Reddy EP, Smirniotis PG (2005) Parametric study of Cs/CaO sorbents with respect to simulated flue gas at high temperatures. Ind Eng Chem Res 44:6485–6490
9. Ribeiro R, Grande C, Rodrigues A (2013) Activated carbon honeycomb monolith–zeolite 13× hybrid system to capture CO_2 from flue gases employing electric swing adsorption. Chem Eng Sci 104: 304–318
10. Anbia M, Hoseini V (2012) Development of MWCNT@ MIL-101 hybrid composite with enhanced adsorption capacity for carbon dioxide. Chem Eng J 191:326–330
11. Anbia M, Hoseini V, Mandegarzad S (2012) Synthesis and characterization of nanocomposite MCM-48-PEHA-DEA and its application as CO_2 adsorbent. Korean J Chem Eng 29:1776–1781
12. Upendar K, Kumar ASH, Lingaiah N, Rao KR, Prasad PS (2012) Low-temperature CO_2 adsorption on alkali metal titanate nanotubes. Int J Greenh Gas Control 10:191–198
13. Lee ZH, Lee KT, Bhatia S, Mohamed AR (2012) Post-combustion carbon dioxide capture: evolution towards utilization of nanomaterials. Renew Sustainable Energy Rev 16:2599–2609
14. Choi S, Drese JH, Jones CW (2009) Adsorbent materials for carbon dioxide capture from large anthropogenic point sources. ChemSusChem 2:796–854
15. Foley HC (1995) Carbogenic molecular sieves: synthesis, properties and applications. Micoporous Mater 4:407–433
16. Lee J, Kim J, Hyeon T (2006) Recent progress in the synthesis of porous carbon materials. Adv Mater 18:2073–2094
17. Ishibashi N, Yamamoto K, Wakisaka H, Kawahara Y (2014) Influence of the hydrothermal pre-treatments on the adsorption characteristics of activated carbons from woods. J Polym Environ 22:267–271
18. Anbia M, Moradi SE (2009) Removal of naphthalene from petrochemical wastewater streams using carbon nanoporous adsorbent. Appl Surf Sci 255:5041–5047
19. Anbia M, Dehghan R (2014) Functionalized CMK-3 mesoporous carbon with 2-amino-5-mercapto-1, 3, 4-thiadiazole for Hg (II) removal from aqueous media. J Environ Sci 26:1541–1548
20. Jong L, Peterson SC, Jackson MA (2014) Utilization of porous carbons derived from coconut Shell and wood in natural rubber. J Polym Environ 22:289–297
21. Ryoo R, Joo SH, Jun S (1999) Synthesis of highly ordered carbon molecular sieves via template-mediated structural transformation. J Phys Chem B 103:7743–7746
22. Xu X, Song C, Andresen JM, Miller BG, Scaroni AW (2003) Preparation and characterization of novel CO_2 "molecular basket" adsorbents based on polymer-modified mesoporous molecular sieve MCM-41. Micropor Mesopor Mat 62:29–45
23. Hiyoshi N, Yogo K, Yashima T (2004) Adsorption of carbon dioxide on amine modified SBA-15 in the presence of water vapor. Chem Lett 33:510–511
24. Xing W, Qiao S, Ding R, Li F, Lu G, Yan Z, Cheng H (2006) Superior electric double layer capacitors using ordered mesoporous carbons. Carbon 44:216–224
25. Shao Y, Wang L, Zhang J, Anpo M (2005) Synthesis of hydrothermally stable and long-range ordered Ce-MCM-48 and Fe-MCM-48 materials. J Phys Chem B 109:20835–20841
26. Colilla M, Balas F, Manzano M, Vallet-Regí M (2008) Novel method to synthesize ordered mesoporous silica with high surface areas. Solid State Sci 10:408–415
27. Gregg SJ, Sing KSW, Salzberg H (1967) Adsorption surface area and porosity. J Electrochem Soc 114:279C
28. Ryoo R, Joo SH, Kruk M, Jaroniec M (2001) Ordered mesoporous carbons. Adv Mater 13:677–681
29. Jun S, Joo SH, Ryoo R, Kruk M, Jaroniec M, Liu Z, Ohsuna T, Terasaki O (2000) Synthesis of new, nanoporous carbon with hexagonally ordered mesostructure. J Am Chem Soc 122:10712–10713
30. Hartmann M, Vinu A (2002) Mechanical stability and porosity analysis of large-pore SBA-15 mesoporous molecular sieves by mercury porosimetry and organics adsorption. Langmuir 18: 8010–8016
31. Cao J, Sun JZ, Hong J, Li HY, Chen HZ, Wang M (2004) Carbon nanotube/CdS Core–Shell nanowires prepared by a simple room-temperature chemical reduction method. Adv Mater 16:84–87
32. Wu C-G (1757-1759) Bein T (1994) conducting polyaniline filaments in a mesoporous channel host. Science
33. Vogiatzis KD, Mavrandonakis A, Klopper W, Froudakis GE (2009) Ab initio study of the interactions between CO_2 and N-containing organic Heterocycles. ChemPhysChem 10:374–383
34. Teng H, Hsieh C-T (1998) Influence of surface characteristics on liquid-phase adsorption of phenol by activated carbons prepared from bituminous coal. Ind Eng Chem Res 37:3618–3624